IEEE Access
Multidisciplinary | Rapid Review | Open Access Journal

Received June 29, 2020, accepted July 8, 2020, date of publication July 13, 2020, date of current version July 23, 2020.

Digital Object Identifier 10.1109/ACCESS.2020.3008709

Non-Smooth Dynamics in Energy Market Models: A Complex Approximation From System Dynamics and Dynamical Systems Approach

JOHNNY VALENCIA-CALVO[1,2], GERARD OLIVAR-TOST[1,3], (Member, IEEE), JOSÉ DANIEL MORCILLO-BASTIDAS[4], CARLOS JAIME FRANCO-CARDONA[5], AND ISAAC DYNER[6]

[1]Universidad de Aysén, Aysén 5950000, Chile
[2]Universidad de Medellín, Medellín 050036, Colombia
[3]Universidad Nacional de Colombia, Manizales 170003, Colombia
[4]Universidad de Monterrey, Monterrey 66238, Mexico
[5]Universidad Nacional de Colombia, Medellín 050034, Colombia
[6]Fundación Universidad de Bogotá Jorge Tadeo Lozano, Bogota 110311, Colombia

Corresponding author: Johnny Valencia-Calvo (johnny.valencia@uaysen.cl)

This work was supported in part by the Universidad de Medellín, in part by the Universidad Nacional de Colombia, in part by the Colciencias (the Colombian research council) Posdoctorados Nacionales under Grant 811-2018, in part by the Colciencias under project Modelado y simulación del metabolismo urbano de la ciudad de Bogotá D.C., under Grant 111974558276, and in part by the DIMA, Universidad Nacional de Colombia under project Modelamiento avanzado de mercados de energía eléctrica para toma de decisiones de inversión y establecimiento de políticas, Hermes under Grant 35467.

ABSTRACT This paper reports a general model that describes the supply and demand of electricity in a national market based on the system dynamics (SD) approach. From the resulting SD model, it derives piecewise smooth (non-smooth) differential equations from the nonlinear functions and feedback cycles of the corresponding stock-flow structure. Subsequently, the stability of the equilibrium points and non-smooth dynamics of the SD model are investigated using the dynamical systems theory. Filippov systems are found in the proposed SD model and non-smooth vector fields associated with generators investment decisions are accumulated. Under this combining methodology, the non-smooth dynamics of energy markets that are governed by the supply and demand laws are uncovered mathematically and deeply described. In fact, we extend our investigation results to any energy market model attached to various investment decisions, confirming the generalizability of our research.

INDEX TERMS Complexity, dynamic systems, energy markets, energy policy, Fillipov systems, modeling, non-smooth dynamic, power markets, simulations, system dynamics.

I. INTRODUCTION

The modeling and simulation of electricity markets is a topic of great interest to the scientific community and to society in general. Since the 1990s, the liberalization and proliferation of energy markets has increased the complexity of their dynamics. Gary and Larsen in [1] shows that the complex dynamics of modern electricity markets cannot be captured by traditional econometric models. For this reason, many post-1990 studies have focused on deregularization (see for example [2]–[4]), which analyzes the impact of different policies associated with investment decisions in electricity markets. However, piecewise smooth methodologies (i.e., dynamical systems methodologies designed for analyzing discontinuous or non-smooth systems [5]) were not yet considered as solutions to these complex systems, even though it has been demonstrated that these methodologies are the most suitable approach for a deep system understanding [5].

Electricity markets have been broadly investigated worldwide using a variety of modeling techniques. The strategies and methodologies for modeling electricity markets are comprehensively described in several reviews [6]–[9]. Power-market dynamics have been mainly described by econometric, probabilistic and agent-based models, and by techniques such as neural networks, genetic algorithms, stochastic optimization methods, and control theory [9]–[12].

The associate editor coordinating the review of this manuscript and approving it for publication was Giambattista Gruosso.

The literature shows three well-developed trends in electricity-market modeling: optimization, simulation, and forecasting. The second trend, which focuses on the general behavior of the system, has gradually gained acceptance by energy specialists as it provides a holistic overview. The complex phenomena of modern energy markets are well captured by systems-thinking tools; accordingly, system dynamics (SD) studies have become ubiquitous in the energy field [9], [13], [14].

The SD approach successfully captures the behavior of the feedbacks from a series of causal relationships that define a given fact based on its main decision-making processes [15]. Classical policy and scenario analyses have proven useful for explaining the different feedback loops in electricity markets [2], [16]. The SD approach combines mathematical modeling with numerical simulation methods. A SD model is generally represented by a set of differential equations that allows an analytic study or a dynamic systems (DS) analysis [17].

On the other hand, piecewise smooth (i.e., discrete- or continuous-time dynamical system whose phase space is partitioned in different regions, each associated to a different functional form of the system vector field [5]) and hybrid dynamical systems (i.e., systems involving both continuous and discrete behaviors [18]) are increasingly used in engineering and applied sciences to model a wide variety of physical systems and technological devices. Examples are mechanical systems with friction and impacts [19], walking robots [20], genetic regulatory networks [21], power electronic converters [22]–[24], hybrid control systems [25], systems with backlash [26], and saturation phenomena. Piecewise smooth dynamics have also appeared in economics and social science, mainly in sustainability development [27], bio-economics [28], and electricity markets [29]–[31]. More generally, any system or device whose dynamics are affected by discontinuous events occurring on macroscopic timescales can be described as a piecewise smooth dynamical system (e.g., see [32], [33]).

The phase space of a piecewise smooth dynamical system is typically divided into several regions associated with different functional forms of its vector field. Such a system can be classified by its degree of discontinuity across the switching manifolds dividing the different regions. Namely, the state trajectories can be discontinuous across manifolds (as in impacting systems), or continuous across manifolds but with discontinuous vector fields (as in so-called Filippov systems). A system can also be piecewise smooth continuous (PWSC), meaning that both its states and vector fields are continuous across the phase space switching manifolds, but with discontinuities of higher order.

PWSC, Filippov and impacting systems exhibit a wide range of nonlinear complex phenomena, including bifurcations and chaos [34], [35]. As the parameters are varied, the phase portrait can lose its structural stability through classical bifurcations such as Fold and Hopf bifurcations. In addition, when an invariant set (equilibria, limit cycles, or other) interacts with a switching manifold in the systems phase space, very different bifurcation phenomena (mainly discontinuity-induced or non-smooth bifurcations) are observed. In this case, the system can exhibit significant transitions from one attractor to another.

Most of the previous works have focused on analyzing and classifying non-smooth bifurcations in piecewise smooth systems. Discontinuity-induced bifurcations of limit cycles in continuous-time piecewise smooth systems have received special attention [5], [36]. Complex dynamics in these kinds of systems are often attributed to grazing bifurcations of the limit cycles [36] (grazing is said to occur when a limit cycle tangentially impacts a switching manifold in the phase space).

Discontinuity-induced bifurcations of equilibria in piecewise smooth flows have also been studied [36]. The structural stability of boundary equilibria (which lie on the switching manifold in the phase space) has been investigated only in specific, low-dimensional PWSC or Filippov systems [37], [38]. Bernardo and Vasca in [39] show that several bifurcation scenarios can occur in such systems, including transitions from equilibria to limit cycles whose amplitude scales linearly with the parameter variation.

In most of the theoretical studies, a manifold divides the state space into two regions with different properties. This is usually justified, as most of the more complicated problems can be locally reduced to this situation. Systems involving more than two manifolds are scarcely reported in the literature because the number of different regions increases exponentially with manifold number, so the analysis becomes quite cumbersome.

To analyze the many applications facing the multi-manifold situation [40], [41], one must resort to numerical simulations. The type of modeling technique and degree of complexity required to capture the features of the real system are widely discussed, as they depend on the needs of the modeler, the phenomena to be represented, and the expected results [42].

It is worth highlighting that the SD and DS approaches are complementary tools that further our understanding of qualitative system behaviors. A combined SD and DS methodology exploits the modern theory of nonlinear DS to describe complex behaviors [12], [17], [29], [30], [35]. However, distinguishing between the qualitative and quantitative properties of complex systems has eluded SD researchers for several years. The term qualitative has different connotations in the DS and SD fields [17]. Although the information contained in time-series data is qualitative in nature, it cannot be considered merely as qualitative. In SD, qualitative refers to the various phenomena that a system can exhibit under uncertainty; that is, the behavioral trends of its dynamic flow over time when the system is after by disturbances. In a SD model, one can study not only the qualitative properties of the system, but also its quantitative results [43], [44].

In this work, the non-smooth properties of a general electricity market are mathematically uncovered and described. As previously stated, other researchers have not fully exploited the DS methodologies in SD models from an

analytical point of view [12], [17], [29], [30]. As a result, the non-smooth properties of energy markets have been barely described and Filippov dynamics have never been found. Against this background, the present paper mathematically analyzes the set of differential equations in a SD model of a general electricity market. The complex dynamics exhibited by such economic models are determined and the results are generalized to other power markets.

The remainder of the paper is organized as follows. Section II is devoted to the modeling and explanation of the system equations describing a general electricity market. This section also discusses the stability of the system. Section III presents the numerical results that motivate the generalization. Section IV performs the piecewise analysis and generalizes the proposed model of the electricity market. Discussions and main conclusions are presented in Section V.

II. NATIONAL ELECTRICITY MARKET MODEL

A. THE SD APPROACH

The SD modeling is a perspective and set of conceptual tools that enable us to understand the structure and dynamics of complex systems as well as to build formal computer simulations of complex systems and use them to design more effective policies and organizations [15]. The SD modeling process has been well documented and readers can find more detail in the work by [15].

This section explains the main elements comprising the general energy market model. First, let us introduce the causal loop diagram (Fig. 1), which incorporates two feedback loops associated with the supply-and-demand sides. To capture the economic nature of energy markets, the loop related to the demand side is inelastic, while the loop associated with the supply side can significantly affect the market dynamics. In this sense, the supply loop is also known as a control loop [14].

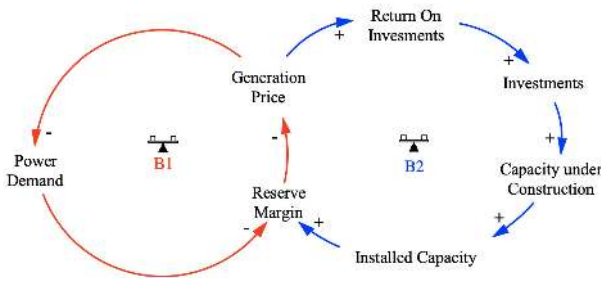

FIGURE 1. Global aspects of the electricity-market model. This causal diagram represents the dynamic hypothesis based on the supply-and-demand laws of power markets. The present paper investigates the interaction between the supply side (loop B_1) and the demand side (loop B_2) of the market. Retrieved from [14], [45].

The dynamic hypothesis of Fig. 1 was retrieved from the work of [14] and [45]. The authors argued that the causal loop diagram explains the fundamental elements of an electricity market. Loops B_1 and B_2 represent the demand and supply sides of the energy market, respectively. In loop B_1, the power demand inversely depends on the generation price or market price, which in turn depends on the system reserve margin. As a measure of the system security, the reserve margin specifies the available capacity above the capacity that meets the power demand, so is essentially determined by the supply-demand relationship. As evident in Fig. 1, the reserve margin negatively affects the generation price. As the reserve margin increases, consumers will pay a lower generation price. Subsequently, the generation price negatively affects the power demand. When the generation price rises, the power demand reduces and vice-versa. Finally, if the power demand decreases, the reserve margin increases. Accordingly, loop B_1 becomes a negative (or balance) loop.

Loop B_2 in Fig. 1 represents the supply side of the market, which mainly depends on the available installed capacity. In other words, loop B_2 illustrates the adjustment of the installed capacity through investment decisions, which in turn depends on the dynamics of the investment returns. If the generation price increases, the return on the investment also increases. The return on investment can be used as a profit measure involving the generation costs and the benefits received. It also motivates the suppliers to build new capacities; as the investment return increases, the capacity under construction enlarges. After a certain period, a greater installed capacity boosts the reserve margin. The dynamics of the general power market manifests as an interaction between the supply-and-demand loops, both linked by a bridge formed by the reserve margin and generation price.

According to SD theory, the attributes that become the level (stock) variables or state (information-storing) variables, the valve or flow variables (variables that represent the rate of information change), the auxiliary variables (variables used for information transformation or intermediate calculations), and the parameters can be derived from the casual loop diagram. In this interpretation, the causal diagram becomes a Forrester diagram or stock-flow diagram [15]. The stock-flow diagram derived from Fig. 1 is shown in Fig. 2, and further explanation of all variables can be found in [12], [29], [30], [45].

The model in Fig. 2 can be written as a system of differential equations with the following state variables (in megawatts):

Installed Capacity.

Capacity under Construction.

Power Demand.

As shown in Fig. 2, the rate of change of Installed Capacity depends on the number of finished plants and the decommission or retirement of old ones. The rate of finished plants is the ratio of the Capacity under Construction to the average time of building a new plant, here called the construction time (in years). Similarly, the retirement rate of old plants is the ratio of the Installed Capacity to the plant lifetime. The first differential equation, which drives the Installed Capacity dynamics, is accordingly written as (1), as shown at the bottom of the next page.

Meanwhile, as illustrated in Fig. 2, the Capacity under Construction is determined by the building rate of new plants,

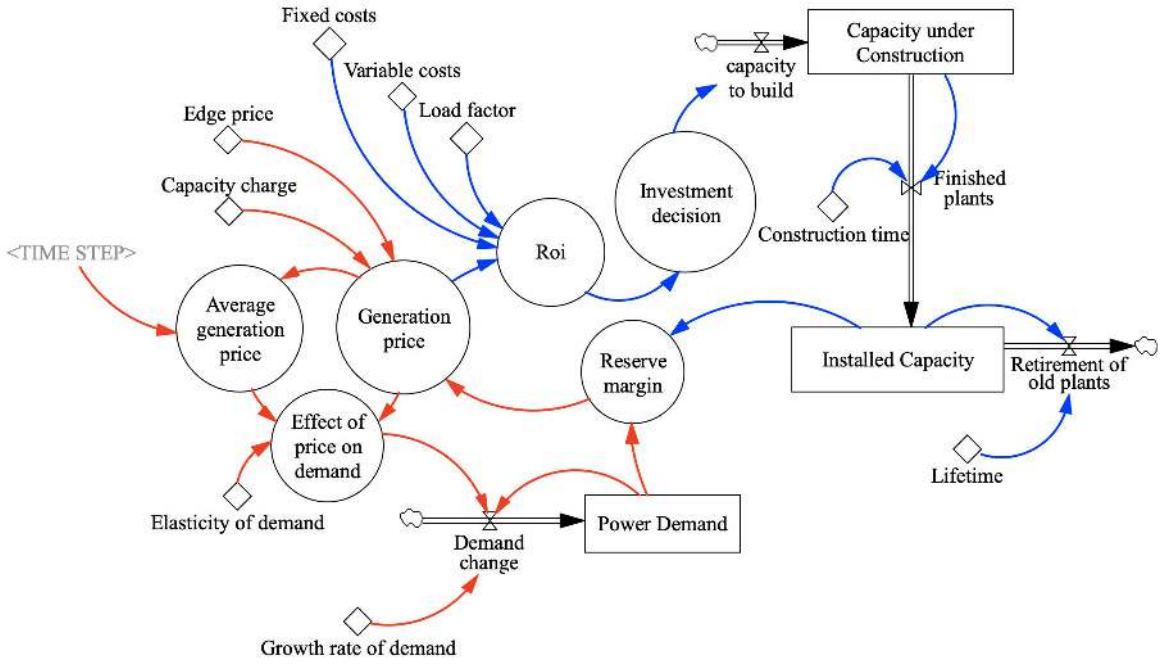

FIGURE 2. Stock-flow diagram of a general electricity-market model derived from Fig. 1 as in [30], [45]. The stock or state variables are Power Demand, Capacity under Construction, and Installed Capacity. The red and blue connectors indicate the information fluxes of the demand and supply sides, respectively. All variables are well explained in [12], [29], [30], [45].

or the capacity to build, and the rate of finishing the plants. The rate of building new plants is represented by a step function that depends on the investment decision, which in turn depends on the return on investment. The return on investment is an income measure including the benefits received and costs incurred in generating a given amount of megawatts. The second differential equation, which drives the Capacity under Construction dynamics, is accordingly written as (4), as shown at the bottom of the next page.

Additionally, the demand creation (the demand change in Fig. 2) defines the rate of change of the state variable Power Demand, which directly depends on attributes such as population growth, industrial activity increase, and the annual increase in demand. All of these attributes are embodied in the demand growth rate, which is also influenced by the effect of price on demand. In the model, the price effect on demand is represented by the generation price over the Power Demand: when the generation price increases the power demand reduces, and vice-versa. The effect of price on demand is also determined by the elasticity of demand (an economic term that measures the demand variation in response to a price change) and the average generation price (a model variable that estimates the weighted average variation of the generation price with respect to the maximum generation price). It is also worth mentioning that both the generation price and return on investment are determined by parameters commonly used in power markets, such as the capacity charge, edge price, fixed and variable costs, and load factor.

The third and last differential equation, which drives the Power Demand dynamics, is accordingly given in (6) and (7), as shown at the bottom of the next page.

Finally, the whole electricity market can be modeled by the set of differential equations as in (8), as shown at the bottom of the next page. The details of this mathematical model will be expanded in the following subsection.

$$\frac{d(Installed\ \ Capacity)}{dt} = Finished\ \ plants - Retirement\ \ of\ \ old\ \ plants \tag{1}$$

where

$$Finished\ \ plants = \frac{Capacity\ \ under\ \ Construction}{Construction\ \ time} \tag{2}$$

and,

$$Retirement\ \ of\ \ old\ \ plants = \frac{Installed\ \ Capacity}{Lifetime} \tag{3}$$

B. MATHEMATICAL MODEL DESCRIPTION

First, the capacity to build, which determines the Capacity under Construction in (8), is defined by a piece wise-smooth function representing the magnitude of the investments (in MW) associated with the rate of building new plants (9), as shown at the bottom of the page. As shown below, the capacity to build is a function of the Installed Capacity and Power Demand, where b_0, b_1 and b_2 are 0, 250 and 750 MW/yr, respectively. Note that the investments in a new capacity represent the capacity installation rate per year, so the unit is MW/yr.

The investment decision, which represents the decided investment in new capacity in the model, depends directly on the magnitude of the revenues or the market share of each utility. As this variable cannot be negative and must meet the return on investment, it is given by

$$Investment\ decision = \max(0, Return\ on\ investment) \quad (10)$$

In equation (10), the return on investment evaluates the efficiency of the capacity investments. This performance measure strongly depends on the generation price in (11), as shown at the bottom of the next page.

Note that the return on investment is also influenced by the fixed and variable costs associated with the generation price paid to the generators. This equation can also include incentives associated with various generation technologies, enabling the evaluation of policies that reduce carbon emissions, improve the supply capacity, or provide other benefits.

The generation price responds to changes in the reserve margin but is limited by the edge price (A) and the capacity charge (B) (see Fig. 3). The generation price is maximized ($A + B$) when the reserve margin is close to zero and minimized (capacity charge - B) when the reserve margin is highest. This is mathematically expressed as:

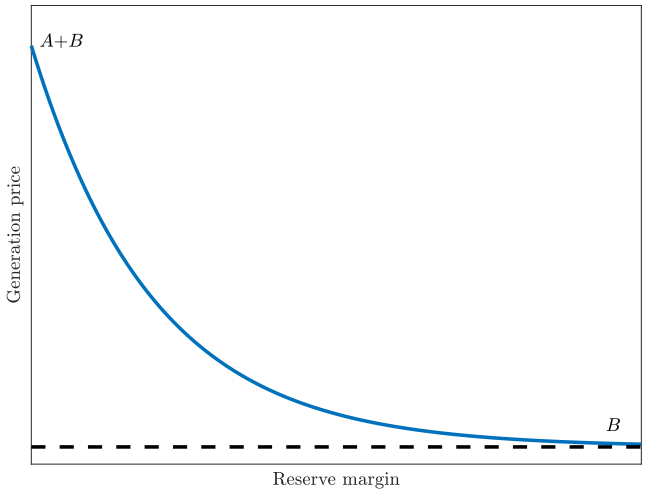

FIGURE 3. Generation price versus reserve margin in an electricity market.

We emphasize that as (12), as shown at the bottom of the next page, represents the real dynamics of the generation price, the sum $A + B$ determines the maximum generation price, while B represents the minimum price (capacity charge). Both prices are designed to limit the generation price under extreme conditions of the reserve margin. Moreover, the values of the generation price and its parameters (A and B) were derived from the real generation-price dynamics of the Colombian power market during the last nine years [46]. In these dynamics, the recurring maximum and minimum prices were approximately 350 and 35 Colombian pesos (COP)/kWh, respectively.

$$\frac{d(Capacity\ under\ Construction)}{dt} = Capacity\ to\ build - Finished\ plants \quad (4)$$

where

$$Capacity\ to\ build = f\ (Investment\ decision) \quad (5)$$

$$\frac{d(Power\ Demand)}{dt} = Demand\ creation \quad (6)$$

where

$$Demand\ creation = (Effect\ of\ price\ on\ demand \times Growth\ rate\ of\ demand \times Power\ Demand) \quad (7)$$

$$\begin{cases} \dfrac{d(Installed\ Capacity)}{dt} = -\dfrac{Installed\ Capacity}{Lifetime} + \dfrac{Capacity\ under\ Construction}{Construction\ Time} \\ \dfrac{d(Capacity\ under\ Construction)}{dt} = -\dfrac{Capacity\ under\ Construction}{Construction\ Time} + Capacity\ to\ build \\ \dfrac{d(Power\ Demand)}{dt} = Effect\ of\ price\ on\ demand \times Growth\ rate\ of\ demand \times Power\ Demand \end{cases} \quad (8)$$

$$Capacity\ to\ build = \begin{cases} b_0 & \text{if } Investment\ decision \leq 0 \\ b_1 & \text{if } 0 < Investment\ decision \leq 0.1 \\ b_2 & \text{if } Investment\ decision > 0.1 \end{cases} \quad (9)$$

The reserve margin is synonymous with the reserve capacity, which measures the available capacity above the capacity that meets the normal peak demand levels. In energy production, the reserve margin is the producer's capacity to generate more energy than the system typically requires. Furthermore, to satisfy the regulatory bodies, the producers must usually maintain a constant reserve margin (between 10 and 20%) as capacity insurance against breakdowns in the electricity system or sudden increases in energy demand. The reserve margin is accordingly defined in (13), as shown at the bottom of the page, for $Installed\ Capacity \neq Power\ Demand$.

As explained above, the reserve margin includes a reliability threshold parameter. Below the reliability threshold, the system must establish restrictions to avoid power outages. In Colombia, the reliability threshold is 0.1 (10%). On the other hand, when the power demand is zero, 100% of the power in the system is available. In a real power market, if Power Demand < Installed Capacity, the system operates under the desired conditions; conversely, if Power Demand > Installed Capacity, the system must restrict its connection services to meet the limited power availability.

Finally, the effect of price on demand in (8) is calculated by (14), as shown at the bottom of the page. The price-and-demand dynamics are further explained in [47], where the generation price is a nonlinear function of the reserve margin. In general, $\frac{Generation\ price}{Average\ generation\ price} \cong 1$, as shown in (15), as shown at the bottom of the page.

TABLE 1. Description of variables and parameters in the power-market dynamics model.

Symbol	Equivalence	Units	Name
r	$\frac{1}{Lifetime}$	$\frac{1}{years}$	Lifetime of the generation plants
q	$\frac{1}{Construction\ time}$	$\frac{1}{years}$	Construction time of the plants
A		COP/kWh	Edge price
FC		COP/kWh	Fixed costs
VC		COP/kWh	Variable costs
LF		%	Load factor
ϵ		%	Elasticity of demand
B		COP/kWh	Capacity charge
k		$1/year$	Growth rate of demand
ω		%	Reliability threshold
inv	(10)	COP	Investment decision
b	(9)	MW/y	Capacity to build
roi	(11)	COP	Return on investment
rm	(13)		Reserve margin
$pgen$	(12)	COP/kWh	Generation price
P	$\overline{pgen}$	COP/kWh	Average generation price
α	(15)		Effect of price on demand

C. QUALITATIVE ANALYSIS: THE DS APPROACH

The DS modeling process, mainly applied in physical systems, involves obtaining the ordinary differential equations of a system and then using them to describe its behavior. Many methodologies have been developed to study dynamic systems, especially from a mathematical perspective [5], [48]. Here, from the SD model it is derived a set of differential equations to transform the SD model into a DS model.

This subsection analyzes the above mathematical model in detail. For this purpose, we rewrite (8) in a compact form using the notation of Bunn, Larsen and Aracil [2], [17]. The parameter values of (8) are listed in Table 1 and the state variables were redefined as follows: Installed Capacity $= x_1$, Capacity under Construction $= x_2$ and Power Demand $= x_3$. The compact set of dynamic equations is given by (16).

$$\begin{cases} \dot{x}_1 = -rx_1 + qx_2 \\ \dot{x}_2 = -qx_2 + b \\ \dot{x}_3 = \alpha k x_3. \end{cases} \tag{16}$$

In this subsection, we compute the local stability characteristics of several equilibrium points arising in the system dynamics model. This is a necessary first step for a global qualitative analysis. We then find the critical parameters in different power-market scenarios. This process is important for setting the operating range and determining the robustness of the system, besides being a fundamental part of the model validation.

$$Return\ on\ investment = \frac{Load factor\ (Generation\ price - Variable\ costs) - Fixed\ costs}{Fixed\ costs} \tag{11}$$

$$Generation\ price = \frac{Edge\ price}{e^{Reserve\ margin}} + Capacity\ charge \tag{12}$$

$$Reserve\ margin = \frac{Installed\ Capacity - Power\ Demand}{Power\ Demand} + Reliability\ threshold \tag{13}$$

$$Effect\ of\ price\ on\ demand = \left(\frac{Generation\ price}{Average\ generation\ price}\right)^{Elasticity\ of\ demand} \tag{14}$$

for $Average\ generation\ price \neq 0$. Therefore,

$$Effect\ of\ price\ on\ demand \cong (1)^{Elasticity\ of\ demand} \tag{15}$$

The equilibrium points in the dynamic equations (16) were obtained as:

$$x^* = \left(\frac{b}{r}, \frac{b}{q}, 0\right) \quad \text{for} \quad k \neq 0, \tag{17}$$

$$x^* = \left(\frac{b}{r}, \frac{b}{q}, x_3\right) \quad \text{for} \quad k = 0. \tag{18}$$

Note that k encompasses three possible scenarios in a real electricity market. When $k > 0$ and $k < 0$, the energy demand of the electricity market follows an usual exponential growth and an exponential decrease, respectively; the latter case explains the gradual increases of prosumers, which reduces the energy demand. Meanwhile, when $k = 0$, the electricity market experiences a lack of energy demand, either because the consumers become prosumers with no need to connect to the network, or remain connected but barely source the electricity from the network. The latter situation has already occurred in California (U.S.), and in parts of Germany, Sweden, and Australia [49], [50]. This case is obviously non-trivial and is worthy of future research.

Furthermore, as b is a piecewise smooth function dividing the state space into three regions, (9) yields up to three equilibrium points, which can be real or virtual.

Although we are mainly interested in scenarios that approximate real-life situations, we analyze some trivial situations for completeness. From a mathematical viewpoint, we must analyze all possible scenarios afforded by the system of equations. As mentioned above, this analysis reveals the operating range and robustness of the model, and is a fundamental part of the model validation. Further information on the validation methodology and robustness is provided elsewhere [15], [51], [52].

Now, let us compute the stability of the equilibrium points. After some straightforward algebra, the Jacobian and its eigenvalues are determined as follows:

$$J = \begin{pmatrix} -r & q & 0 \\ 0 & -q & 0 \\ 0 & 0 & k \end{pmatrix} \Rightarrow \begin{matrix} \lambda_1 = \alpha k \\ \lambda_2 = -q \\ \lambda_3 = -r \end{matrix}$$

It is worth to note that, the stability condition is driven by k (the growth rate of demand). Therefore, we varied k within a small (but meaningful in the real world) neighborhood of the origin, and observed the scenarios arising in the system. The first results are presented in Fig. 4.

When the growth rate of demand is positive (Fig. 4(a) - (f)), all the equilibriums are unstable and the state variables exhibit a transient oscillatory behavior that strengthens as k approaches zero. Conversely, when k is negative (Fig. 4(g) - (i)) the equilibriums are stable and their state variables converge to the fixed point (0, 0, 0), previously obtained as (17).

The local stability of the equilibrium points depends on the parameter k. In the three cases presented above, the eigenvalue λ_1 associated with the power demand is unstable for positive values of k and stable for negative k. In the case of negative k, the behavior reaches stable equilibrium at the origin. Note that when k is very close to zero, the number of oscillations increases. Oscillatory behaviors in the power-market system implies that the investment decisions are rapidly changing. In practical terms, $k > 0$ indicates that consumers extract electricity from the network and become part of the electricity system load. Moreover, when $k > 0$ and $x_3 > x_1$ (demand exceeds supply) the system faces a rationing scenario. To avoid blackouts, the decisions in this case must rapidly reduce the demand. As government and policy makers cannot wait for this scenario, they usually impose a reliability threshold (ω) in the electricity markets as an alert indicator, enabling control actions that maintain the reserve margin (rm) at or above ω well in advance. To accomplish this complicated task, government and policy makers must discourage the demand growth through savings policies, planned rationing, higher electricity tariffs, or other deterrents. In other words, ω prevents the rm from reaching zero by immediately alerting the authorities to enact demand reduction policies. Similarly, our proposed model limits the growth of x_3 by imposing a threshold ω, ensuring that demand never exceeds supply. Also note that when $rm < \omega$, especially when $rm < 0$, the SD model undergoes a structural change into a different dynamic system. This case is beyond the scope of the present paper.

On the other hand, $k < 0$ indicates an increasingly off-the-grid scenario initiated by technological and economic changes that challenge and transform the electric utility industry. Such disruptive challenges require a convergence of two factors: falling costs of distributed power generation, and the emergence of other distributed energy resources. The second factor arises when consumers implement self-generation technologies that satisfy their own demands. In response to consumer self-sufficiency, the utility may cease investment in new generation and disconnect some already installed plants. The implications of varying the k parameter will be thoroughly investigated in the next section.

In real cases, the growth rate of demand can switch from positive to negative even on monthly timescales. This behavior is shown in Fig. 5, which depicts the monthly energy demand in Colombia. Note that the growth rate of demand quickly changes from positive to negative as the energy demand increases or decreases from month to month. These behaviors can send wrong signals to electricity investors, in turn affecting the SD model. Such phenomena in power markets justify investigating the behaviors and stabilities of the main system variables while varying k.

III. NUMERICAL RESULTS

In the following, we present and explain the numerical tools and results of the proposed electricity-market model. The analysis is based on the qualitative analysis addressed in the last section. Before running the computer programs, we identified the variables and parameters that influence the SD model by studying the mathematical components of the proposed model.

Three fundamental sensitivity measures are valuable in SD models, namely, the numerical, behavioral and policy

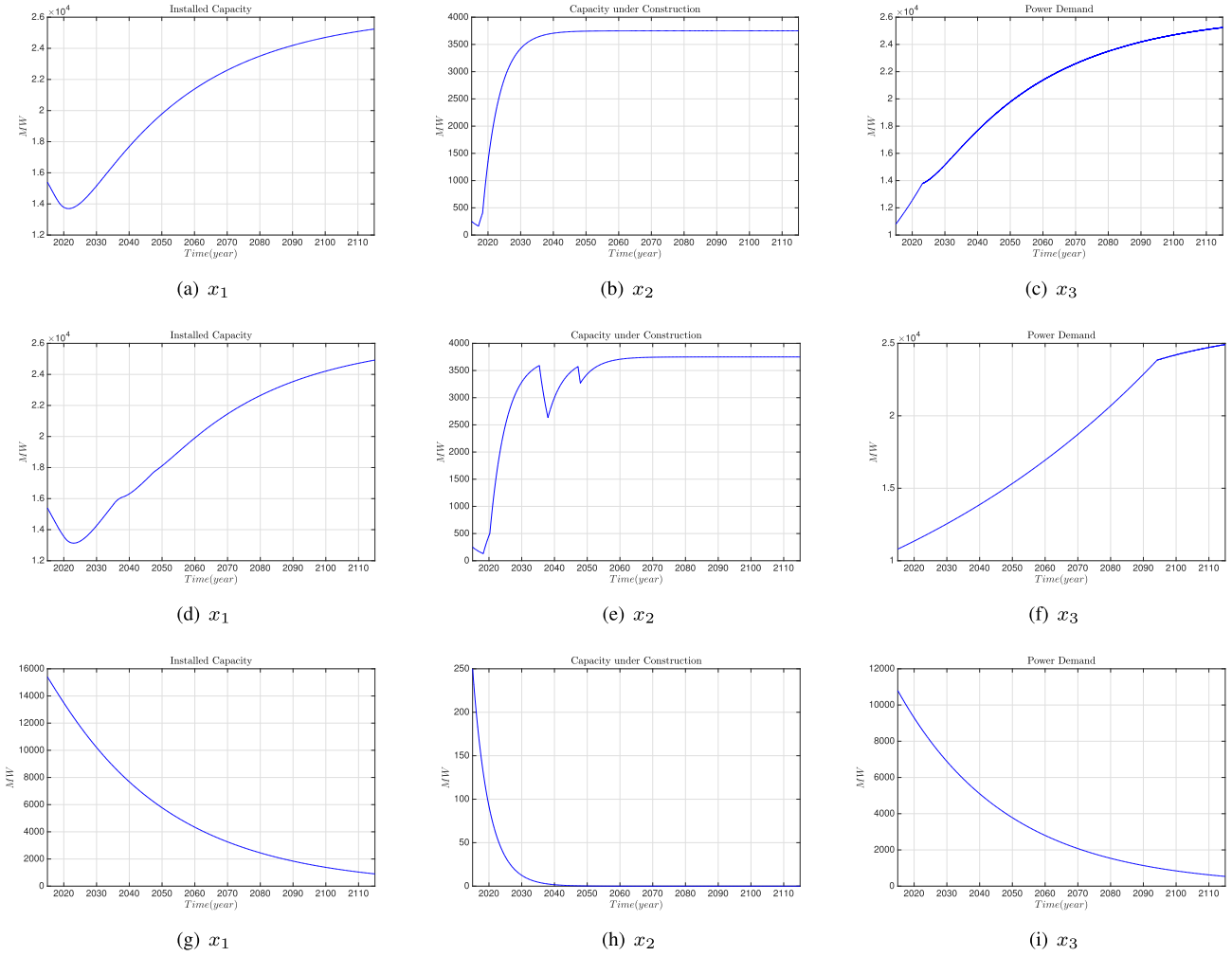

FIGURE 4. Electricity-market dynamics for different k (growth rate of demand). $k = 0.03$ in (a), (b), (c), $k = 0.01$ in (d), (e), (f), and $k = -0.03$ in (g), (h), (i).

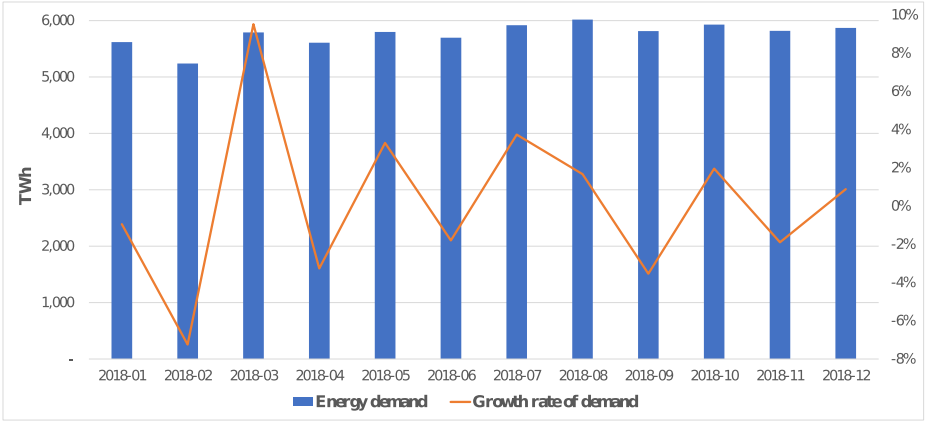

FIGURE 5. Monthly demand dynamics (blue bars) and Colombian growth rate of demand (orange lines). The data were sourced from the XM web page [53].

sensitivities. A model is numerically sensitive when a change in the model assumptions (parameters, manifolds or aggregation) changes the numerical results. For example, changing the elasticity of the word-of-mouth feedback in a diffusion model of new technologies altered the growth rate of the new product. Sterman noted that "all models exhibit numerical

sensitivity [15]". In a behaviorally sensitive model, modifying the assumptions significantly alters the behavior patterns of the model. For instance, the model behavior may transform from weak oscillatory behaviors to smoother but radical behaviors (either increasing or decreasing). Finally, a model is policy sensitive when a change in the hypothesis reverses the impacts or convenience of a proposed policy.

Fig. 6 shows the numerical sensitivity results of the model state variables as the growth rate of demand varies. As previously stated, this parameter significantly affects the behavior of our proposed model. During this analysis, some of the three state variables started declining and oscillating in the beginning stages of the market development, while others increased rapidly or moderately. Depending on the value of k, the power market evolved toward a tipping point or inevitably collapsed. This information might assist policy developers to manage their energy projects under changing demands.

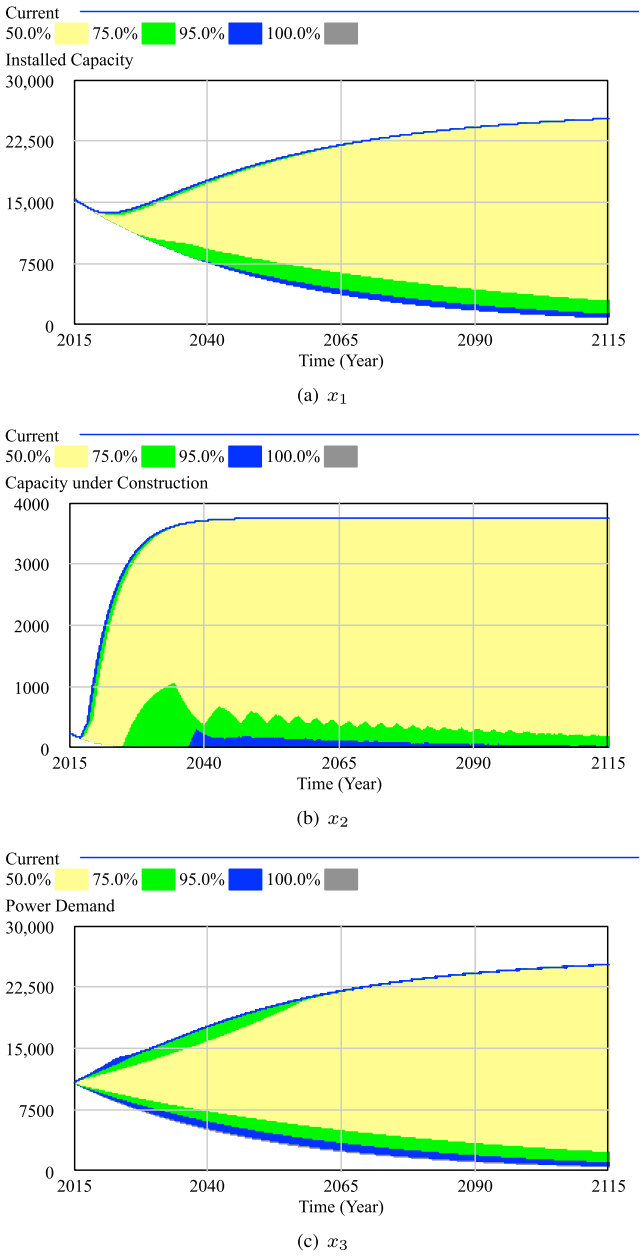

FIGURE 6. Numerical sensitivity result of varying k (growth rate of demand) in the range$(-0.03, 0.03)$.

The individual traces of the sensitivity analysis reveal the full range of the model outcomes (the capacity under construction in Fig. 7) when varying the growth rate of demand. Note that Figs. 6 and 7 clarify only the confidence limits of the runs; the local and detailed information cannot be extracted from this type of sensitivity analysis. Broadly speaking, the classical sensitivity analysis is simply numeric, and does not reveal the modes of the system behavior. Instead, it reveals the behavioral trends of the power market along the whole simulation window in the hypothetical cases of different k.

The numerical sensitivity analysis was computed by the Monte Carlo method incorporated in the VensimPlus simulation package. The simulation window for k ranged from -0.03 to 0.03. Many iterations (more than 2000) were computed to cover a wide spectrum of feasible and consistent solutions. A vector distribution was assumed.

A. ASYNCHRONOUS SWITCHING MAPS

The asynchronous switching map (A-Switching Map) is a tool for studying the complex behaviors of real physical systems, such as power converters [39], pendulum systems [54], and spring-mass systems [55]. A-Switching Map is usually applied to piecewise-smooth DS, and has not previously been implemented to social systems and SD theory. In summary, A-Switching Map is suitable for models represented by a set of ordinary differential equations with discontinuous functions since discontinuities or sudden changes in the system behavior can be easily detected and illustrated. Considering that many systems modeled by the SD approach involve decision-making, and (consequently) discontinuities, they are expected to be well-handled by A-Switching Map. Fig. 8 shows the A-Switching Map result of Capacity under Construction versus k. This map accounts for the discontinuity-associated phenomena from a different perspective not previously observed in SD theory or social systems. By applying the A-Switching Map tool, we can evaluate different alternatives and extract additional information from the model. As indicated in Fig. 8, A-Switching Map samples the state variables at their transitions and steady states after detecting a change in the capacity to build (b) signal. Each sampled value is stored and plotted against its respective k value. Clearly, this methodology can plot either the transient or steady-state values (see Fig. 9).

As a first step, let us investigate the transient state of the possible behaviors when the growth rate of demand k varies. Recall that in our proposed model (see (16)) the capacity under construction (x_2) was dramatically affected by the discontinuous value of the investments (b). Therefore, how the investment decisions affect the capacity under construction is particularly interesting. As shown in Fig. 9(a)-(c),

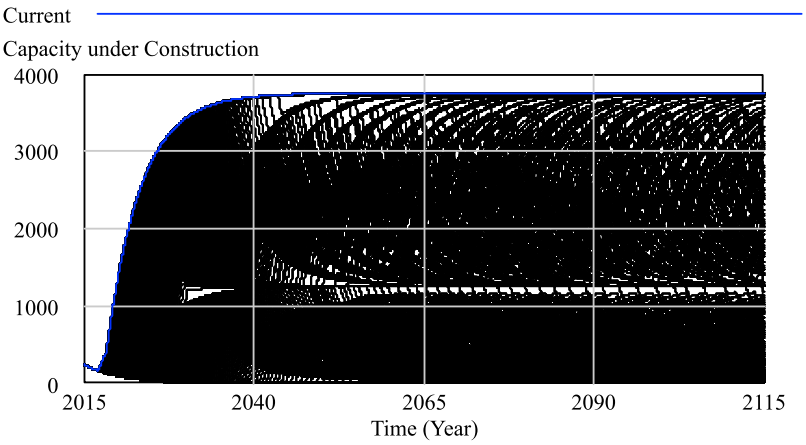

FIGURE 7. Individual time-history evolutions of 2000 simulations in the sensitivity analysis of Capacity under Construction (x_2).

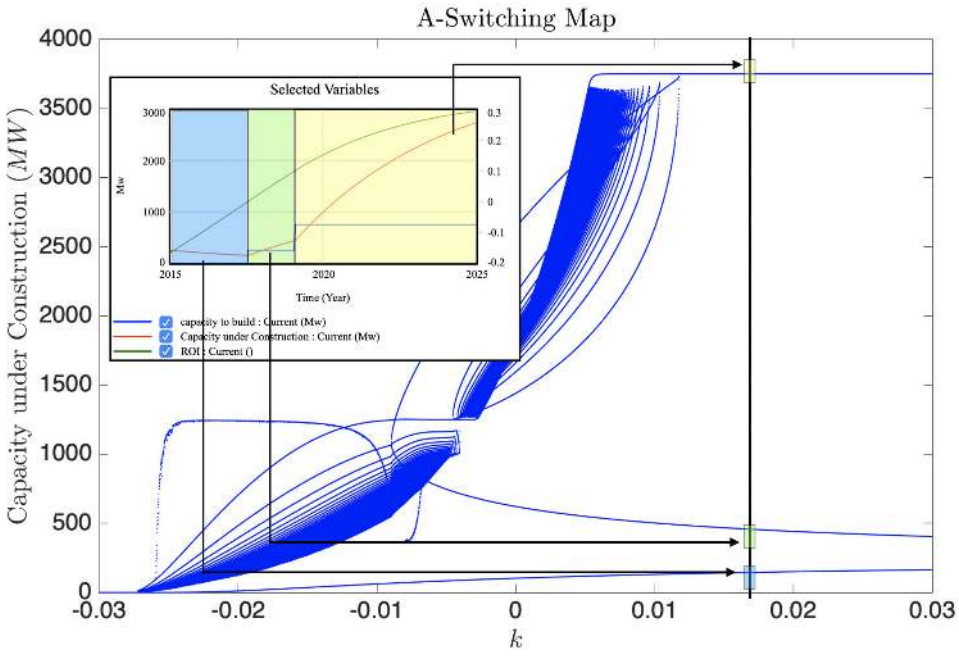

FIGURE 8. Application of the A-Switching Map technique to Capacity under Construction versus k.

numerous scattered points cluster around the interval $k \approx (-0.025, 0.01)$, meaning that in transient state, the capacity to build (b) varies substantially when the growth rate of the demand approaches zero. These projections of the system state variables reveal not only the variable behaviors for specific k values, but also their expansion along the transient trajectory in the solutions map. In the present case, the transient trajectories of all three state variables (x_1, x_2 and x_3) formed a butterfly-wing pattern in the zero-k neighborhood. Note that the mapping determines not merely the confidence limits of the transient trajectories but also their complex dynamics. For instance, the system displays strongly oscillating behavior around $k \approx 0$ and monotonic behavior above 0.015 and below -0.03. It is worth mentioning that these behaviors emerge within the k values of real electricity markets.

The A-Switching Maps of the steady-state results of the growth-rate-of-demand analysis are presented in Fig. 9(d)-(f). These plots reveal the tendency of the system behavior once the transient state has elapsed. In other words, we can establish the equilibrium points of the system state variables over a broad spectrum of k values. Note that in steady state, the oscillations become weaker in the $(-0.025, 0.01)$ range of k, indicating settling to an equilibrium point. Moreover, comparing the results of the transient and steady-state analyses (Fig. 9) with those of the numerical sensitivity analysis (Fig. 6), the maximum and minimum values coincide but the

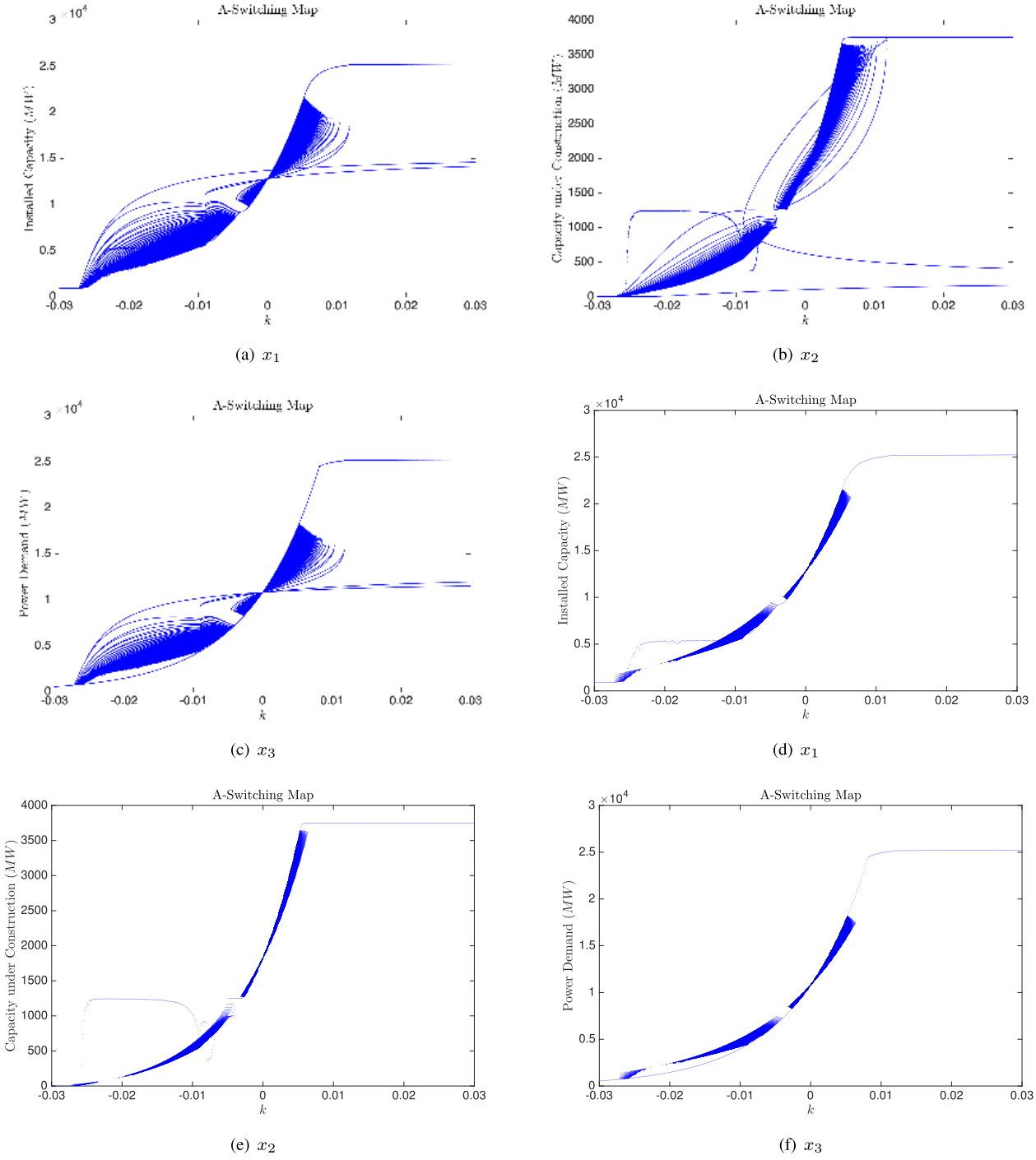

FIGURE 9. A-Switching Map applied to the growth-rate-of-demand analysis in (a), (b), (c) transient state and (d), (e), (f) steady state. k is varied from -0.03 to 0.03.

exact k value at which deterministic behavior emerges cannot be discerned in Fig. 6. In contrast, Fig. 9 indicates the points of accumulation and multiple oscillations. It is worth noting that this analysis is also available for model calibration.

IV. ENERGY MARKET GENERALIZATION

In many research fields, discontinuous dynamical systems are modeled by continuity equations. However, continuum models cannot adequately predict or characterize discontinuous dynamics. To better understand and represent a piecewise-smooth continuous system, one must resort to non-smooth dynamics methodologies. As the complexity of a piecewise-smooth continuous system grows exponentially with the degree of discontinuity, a global piecewise-smooth continuous system should be simplified by dividing it into several continuous subsystems of different domains,

each with different dynamic properties governed by individual rules that link to the adjacent continuous sub-system(s). The transition laws between the borders or subsystems can then be determined and studied in more detail.

By this approach, a generalized system representing the supply-and-demand behavior of a liberalized electricity market was constructed as follows:

$$\begin{cases} \dot{x}_1 = -rx_1 + qx_2 \\ \dot{x}_2 = -qx_2 + b \\ \dot{x}_3 = \alpha k x_3. \end{cases} \tag{19}$$

with $r, q > 0$, $k \in \mathbb{R}$ and

$$b(inv) = \begin{cases} b_0 & \text{if} \quad inv \leq d_0 \\ b_1 & \text{if} \quad d_0 < inv \leq d_1 \\ b_2 & \text{if} \quad d_1 < inv \leq d_2 \\ \vdots & \vdots \qquad\quad \vdots \\ b_{n-1} & \text{if} \quad d_{n-2} < inv \leq d_{n-1} \\ b_n & \text{if} \quad inv > d_{n-1}. \end{cases} \tag{20}$$

To mimic typical real situations, we set $b_0 = d_0 = 0$, and

$$\{b_i\}_{i=1}^{n} \; ; \; b_i > 0 \quad \text{such that} \quad b_0 < b_1 < \cdots < b_n$$
$$\{d_i\}_{i=1}^{n-1} \; ; \; d_i > 0 \quad \text{such that} \quad d_0 < d_1 < \cdots < d_{n-1}$$

The other equations defined above remain unchanged.

Recall that our state variables x_1, x_2 and x_3 refer to the *Installed Capacity*, *Capacity under Construction* and *Power Demand*, respectively. Recall also the system parameters: k is the growth rate of demand, the parameters b_n and d_n are associated with the investment strategy, and the reliability threshold ω (see (13)).

Now consider the system governed by (9) and (16) in Section II under the following parameter settings: $n = 2$, $b_0 = d_0 = 0$, $b_1 = 250$, $b_2 = 750$, $d_1 = 0.1$, $k \in [-0.03, 0.03]$ and $\omega = 0.1$.

Note that due to the discontinuities imposed by the capacity to build (b), the reserve margin (rm) and the investments (inv), our dynamical system can be described by a piecewise smooth set of ordinary differential equations. Therefore, our system can be classified as a Filippov-type system and can be studied by Filippov theory [35].

To geometrically define the different regions in the state space, we first identify the discontinuity types of the variables:

1. ***Reserve margin*** *(rm):* The *rm* induces a discontinuity of the first type (continuous vector field across the switching manifold $\{x_1 = x_3\}$). This is a non-Filippov situation.
2. ***Investments*** $(inv) = max\{0, \; roi\}$: The *inv* also induces a first-type discontinuity.
3. ***Capacity to build*** *(b):* b induces a discontinuity of the second type (discontinuous vector field across the switching manifolds $inv = 0$ and $inv = d_1$). This system is a Filippov-type system that is able to display sliding solutions.

In the following, we analyze the system around the switching manifolds that define the geometrical shapes of the manifolds. In the first non-Fillipov case above, the manifold is defined by (21) and displayed in Fig. 10.

$$\left\{ \Sigma \equiv \left\{ (x_1, \; x_2, \; x_3) \in \mathbb{R}^3 : x_1 - x_3 = 0 \right\}. \right. \tag{21}$$

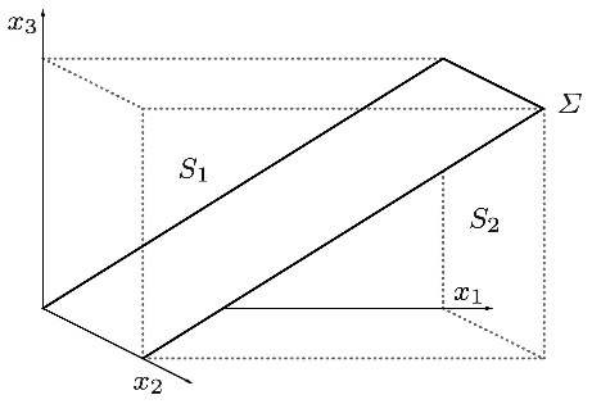

FIGURE 10. Switching manifold Σ in the state space.

The *roi* possibilities are then simply verified as:

$$\begin{aligned} roi > 0 \Leftrightarrow \frac{LF(pgen - VC) - FC}{FC} > 0 \\ \Leftrightarrow pgen > VC + \frac{FC}{LF} \quad (\text{since } FC > 0). \end{aligned} \tag{22}$$

Considering the generation price ($pgen$) in (12), we have

$$B + \frac{A}{e^{rm}} > VC + \frac{FC}{LF} \Leftrightarrow \frac{1}{e^{rm}} > \frac{VC + \frac{FC}{LF} - B}{A},$$

which is feasible when $VC + \frac{FC}{LF} > B$.

Thus, if $VC + \frac{FC}{LF} \leq B$, the *roi* is always < 0 and $b = 0$ with $inv = 0$. Rewriting (19) as (23):

$$\begin{cases} \dot{x}_1 = -rx_1 + qx_2 \\ \dot{x}_2 = -qx_2 \\ \dot{x}_3 = \alpha k x_3. \end{cases} \tag{23}$$

We can analyze the equilibrium points and the stability conditions in each region (labeled S_1 and S_2 in Fig. 10):

- On S_1 ($x_3 > x_1$), we have $rm = \omega$ and $\alpha > 0$.
  Thus, the equilibrium point is located in $x^* = (0, 0, 0)$ and its stability depends on the Jacobian:

$$J = \begin{pmatrix} -r & q & 0 \\ 0 & -q & 0 \\ 0 & 0 & \alpha k \end{pmatrix}$$

  This equilibrium point is asymptotically stable if $k < 0$ or asymptotically unstable if $k > 0$, with $\alpha = \left(\frac{P_{gen}}{P}\right)^{\varepsilon} > 0$ when $P_{gen} = B + \frac{A}{1+e^{\omega}}$.
- On S_2 we obtain ($x_3 < x_1$), $rm = \omega + \frac{x_1 - x_3}{x_3}$ and we approximate $\alpha = \left(\frac{P_{gen}}{P}\right)^{\varepsilon} \approx 1$.

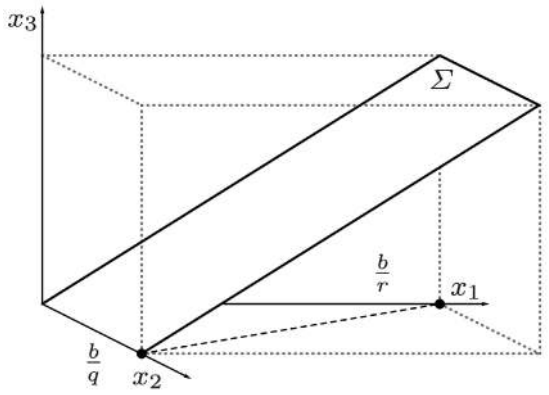

FIGURE 11. Parameter-dependence on b, for the equilibrium points.

Let us consider the case $VC + \frac{FC}{LF} > b$. Here $roi > 0$ and

$$e^{rm} < \frac{A}{VC + \frac{FC}{LF} - B}. \tag{24}$$

Note that when $\frac{A}{VC+\frac{FC}{LF}-B} > 0$, rm is given by

$$rm < \log\left(\frac{A}{VC + \frac{FC}{LF} - B}\right). \tag{25}$$

- ***Subcase*** $x_1 \leq x_3$: $rm = \omega$. Here we have

$$\omega < \log\left(\frac{A}{VC + \frac{FC}{LF} - B}\right). \tag{26}$$

In this case b is a constant that depends on the parameters. The equilibrium point is then given by $x^* = \left(\frac{b}{r}, \frac{b}{q}, 0\right)$, which is always virtual unless $b = 0$. Recall that b is given by (20) with $n = 2$ (see also Fig. 11).

The stability of the equilibrium point depends on the following Jacobian:

$$J = \begin{pmatrix} -r & q & 0 \\ 0 & -q & 0 \\ 0 & 0 & \alpha k \end{pmatrix}$$

The equilibrium point is asymptotically stable and unstable when $k < 0$ and $k > 0$, respectively. This is true because $\alpha = \left(\frac{P_{gen}}{P}\right)^{\varepsilon} > 0$ when $P_{gen} = B + \frac{A}{e^{\omega}}$.

- ***Subcase*** $x_1 > x_3$: In this $rm = \omega + \frac{x_1 - x_3}{x_3}$ case,

$$\omega + \frac{x_1 - x_3}{x_3} < \log\left(\frac{A}{VC + \frac{FC}{LF} - B}\right), \tag{27}$$

$$\frac{x_1}{x_3} < \log\left(\frac{A}{VC + \frac{FC}{LF} - B}\right) + 1 - \omega \equiv \frac{1}{h_1}$$

$$\Leftrightarrow \frac{x_1}{x_3} < \frac{1}{h_1}. \tag{28}$$

Hence, (29) defines another switching manifold (see Fig. 12).

$$\Sigma_1 \equiv \left\{(x_1, x_2, x_3) \in \mathbb{R}^3 : x_1 - h_1 x_3 = 0\right\}. \tag{29}$$

Note that if $roi = 0$, then $inv = 0$ and $b = 0$.
On the other hand, if $roi > 0$, then $inv = roi$. From (11) and (10), we have $inv \equiv inv(x_1, x_3)$. Consequently, $inv < d_1$ and $inv > d_1$, define two new sub-regions in S_2. Like the previous subcase ((29)), this subcase yields a new switching manifold separating the sub-regions (see (31) and Fig. 13).

$$\frac{x_1}{x_3} > \log\left(\frac{A}{FCd_1 + VC + \frac{FC}{LF} - B} - 1\right) + 1 - \omega$$

$$\equiv \frac{1}{h_2} \Leftrightarrow \frac{x_1}{x_3} < \frac{1}{h_2} \tag{30}$$

$$\Sigma_2 \equiv \left\{(x_1, x_2, x_3) \in \mathbb{R}^3 : x_1 - h_2 x_3 = 0\right\} \tag{31}$$

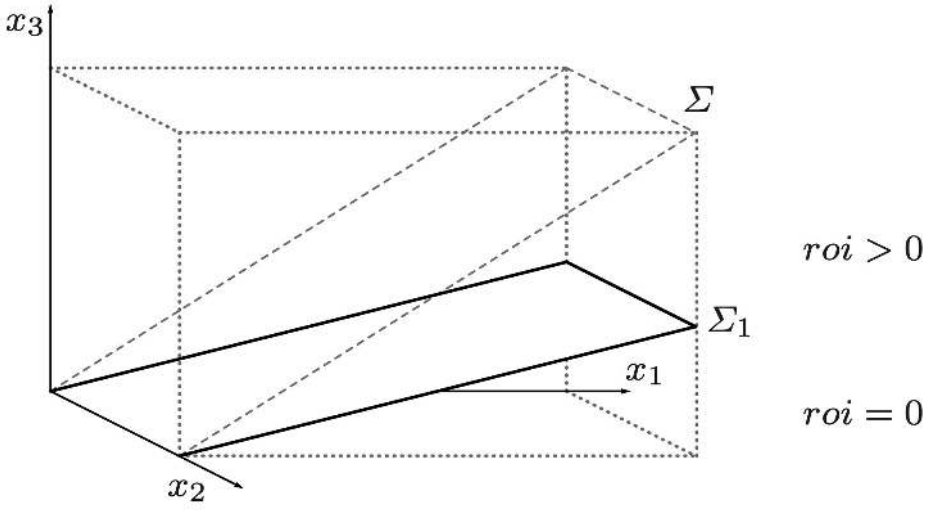

FIGURE 12. Three regions by the switching manifolds Σ_1 and Σ_2.

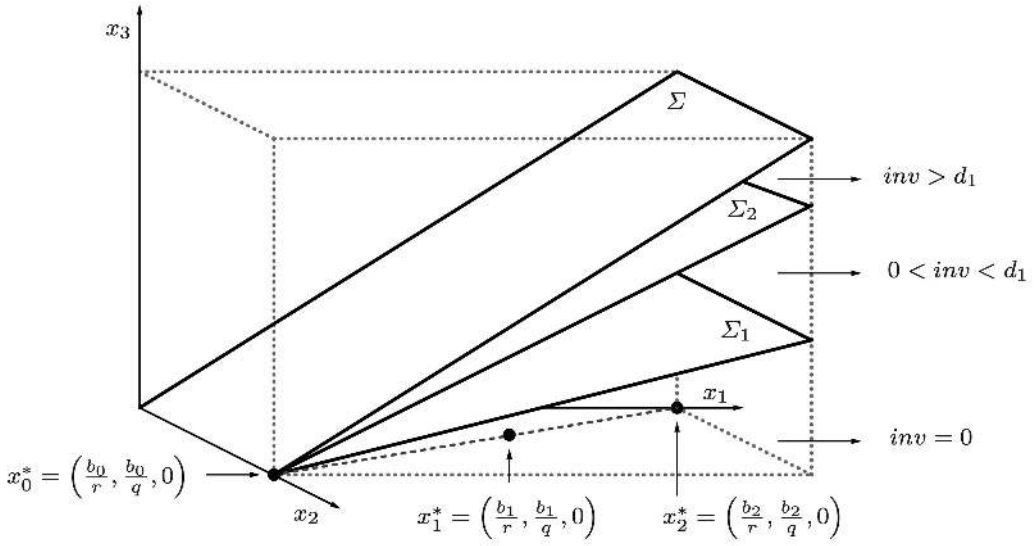

FIGURE 13. Switching manifolds Σ, Σ_1 and Σ_2, and the equilibrium points ($b_0 = 0 < b_1 < b_2$) in the state space.

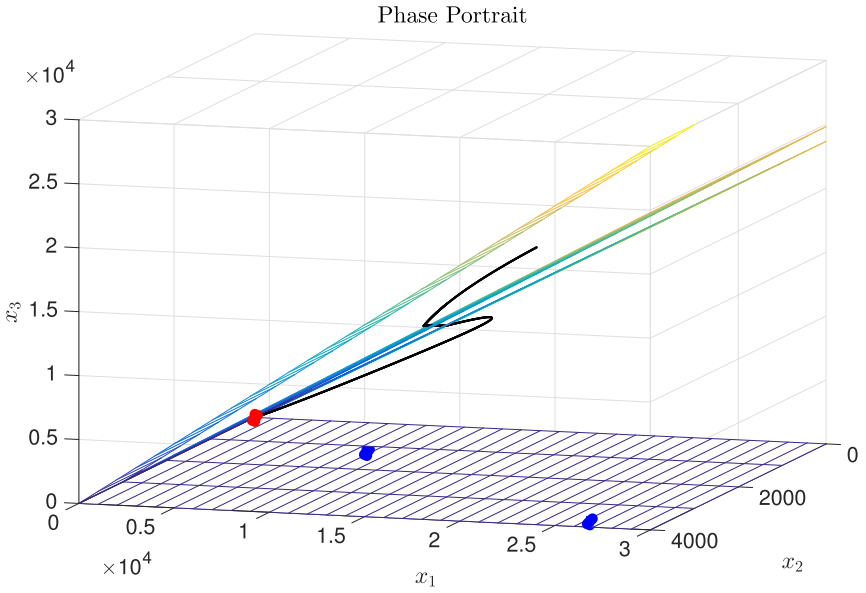

FIGURE 14. General dynamics of the system behavior across the switching manifolds for $k < 0$.

We emphasize that each region contains a virtual equilibrium point that can be asymptotically stable or unstable depending on the stability conditions defined by k. Note also that $h_1 < h_2$, as demonstrated in Appendix.

Moreover, the parameters associated with the slopes of the switching manifolds are related to the return on investment (*roi*). Therefore, through the proposed generalization, we confirmed that the feedback loop B_2 (see Fig. 1) is the control loop. Specifically, we verified that varying the costs (*FC* and *VC*), load factor (*LF*) and capacity charge (*B*) alter the slopes of the switching manifolds. If the system evolves within a defined region under specific initial conditions, then the system behavior can be predicted by understanding the eventual equilibrium point of the system solution.

Fig. 14 is a three-dimensional representation of the system behavior through the switching manifolds under a negative growth rate of the demand k. As the system (black line) evolves, it crosses the Σ_2 and Σ_1 manifolds, invariably following their associated virtual equilibrium points. The evolving system tends to its corresponding equilibrium point, so after crossing a switching manifold, the trajectory changes as the system finds another equilibrium point in the region just entered. This behavior explains the oscillatory dynamics of the system. At the end of the simulation, the system reaches the unique feasible equilibrium point (the red point (0, 0, 0)) in the region beneath manifold Σ_1. Under different initial conditions, the oscillatory dynamics among the manifold can be strengthened because the system is always attracted to

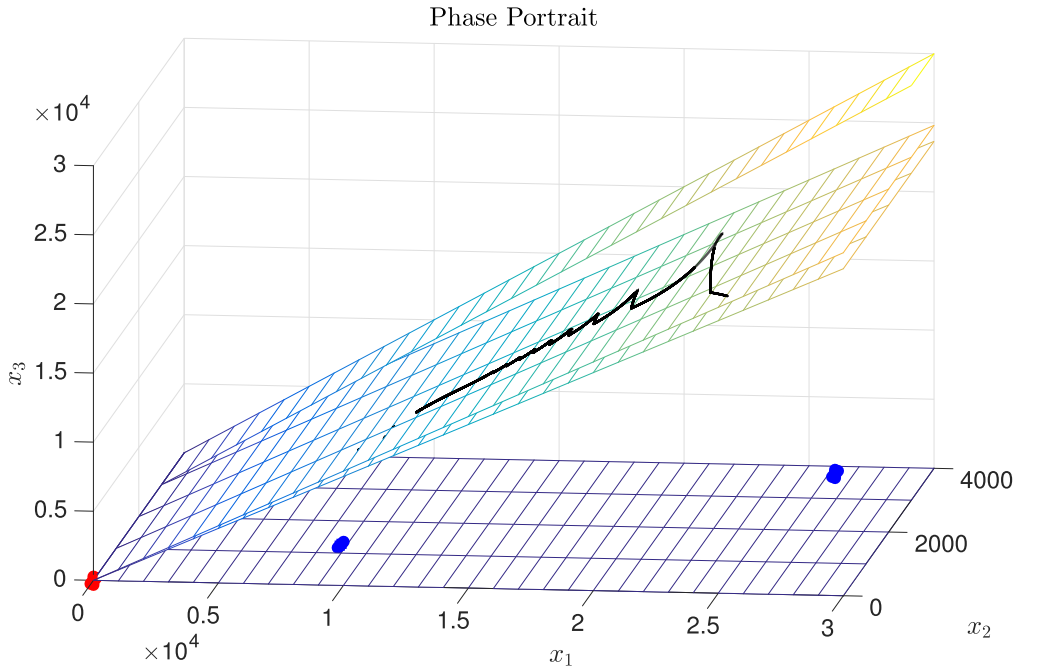

(a) 3D Phase portrait

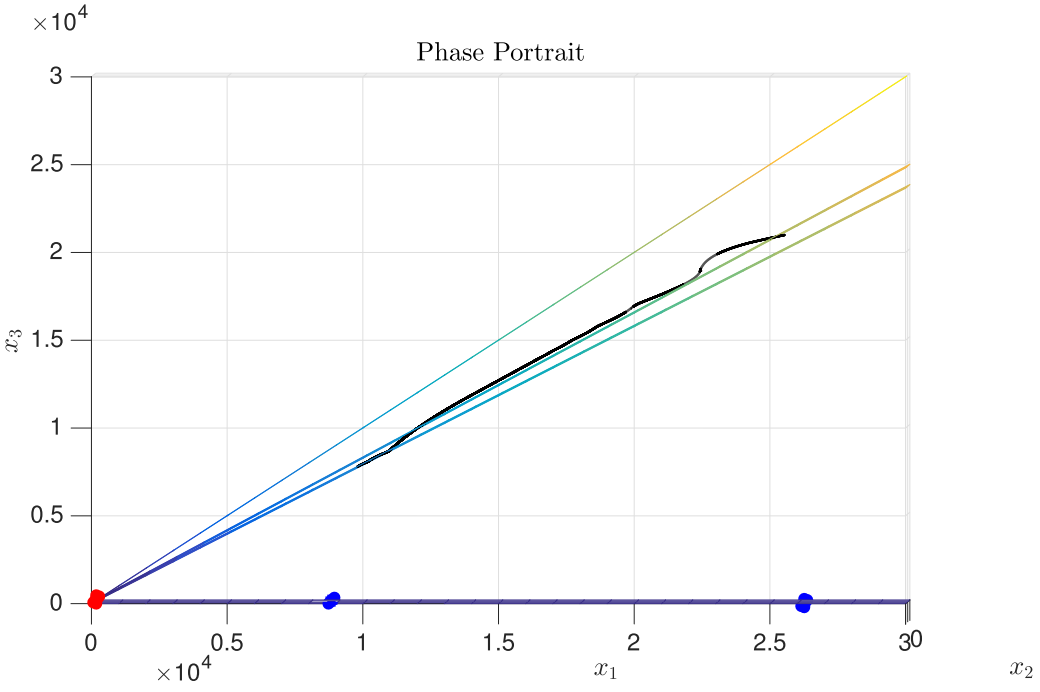

(b) 2D Phase portrait

FIGURE 15. General dynamics of the system behavior across the switching manifolds for $k < 0$. The initial conditions are changed from those of Fig. 14.

the virtual equilibrium in each region, and the manifolds are close one another (see Fig. 15). Note that the system in Fig. 15 oscillates while seeking the equilibrium point in each region it enters. In this case, none of the equilibriums are reached because the simulation horizon is too short. However, lengthening the simulation horizon is nonsensical for practical purposes. A careful examination of Fig. 15 reveals that the system evolves across the switching manifolds in a multiple-crossing mode, which is associated with oscillations in investment decisions. In the next section, the reasons for this complex phenomena are revealed in a Filippov analysis.

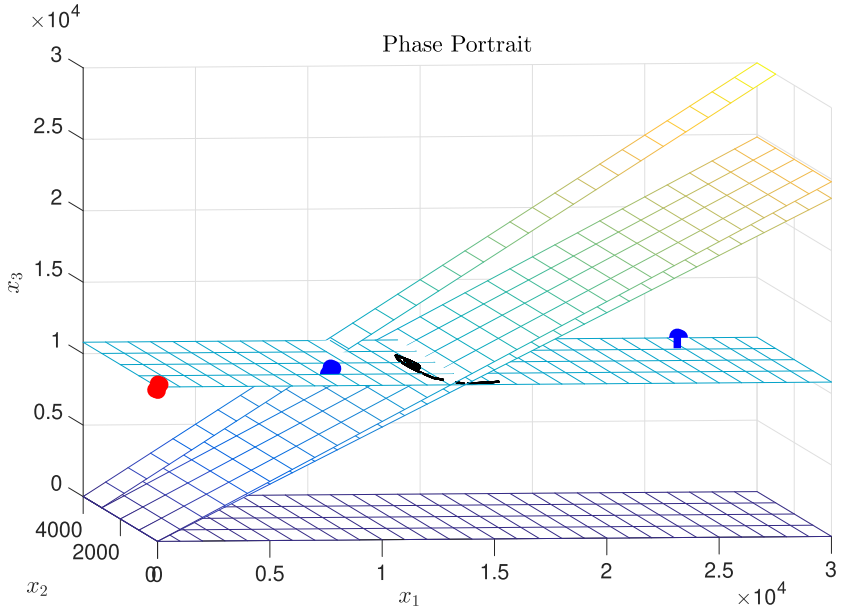

FIGURE 16. General dynamics of the system behavior on the subspace $\{x \in \mathbb{R}^3 : x_3 = h\}$.

Now consider the case $k = 0$ (in which users become prosumers and the generators cease investing in new capacity). In this case, the installed generation plants may become obsolete. Setting $\dot{x}_3 = 0$ in (19), we have $x_3 = x_3(0) = h$, where h is a positive constant ($h > 0$, $h \in \mathbb{R}$). Under this condition, the system behavior evolves in the plane $x_3 = h$, as seen in Fig. 16.

According to Fig. 16 and the above statement, (19) can be rewritten as a planar autonomous system of two differential equations, in which the equilibrium points lie in the plane $x_3 = h$ (see Fig. 16):

$$\begin{cases} \dot{x}_1 = -rx_1 + qx_2 \\ \dot{x}_2 = -qx_2 + b. \end{cases} \tag{32}$$

At this point, we highlight that qualitative analysis in national electricity-market models aids the recognition of parameters or functions that lead the system to certain threshold points. Complementary information can be obtained by performing a sensitivity analysis. Therefore, we can further analyze the models, study several scenarios, and evaluate a broad spectrum of policies.

A. FILIPPOV ANALYSIS

The Filippov method, originally developed for mechanical systems with stick-slip motion, can predict instabilities in piecewise-smooth systems with fast dynamics. Especially, it predicts the parameter range that avoids the first bifurcation of the fast dynamics, i.e., it estimates the stability margins of the system and describes the trajectory evolution [56]–[58]. As discussed in the previous sections, electricity markets are characterized by discontinuous functions leading to complex behaviors. By studying the system behavior through the different switching manifolds, the Filippov method describes the electricity-market dynamics in more detail than conventional analysis [59]–[61]. To this end, we consider the following manifolds:

$$\begin{aligned} \Sigma &\equiv \left\{x \in \mathbb{R}^3 : x_1 = x_3\right\} \\ \Sigma_1 &\equiv \left\{x \in \mathbb{R}^3 : x_1 = h_1 x_3\right\} \\ &\vdots \quad \vdots \\ \Sigma_n &\equiv \left\{x \in \mathbb{R}^3 : x_1 = h_n x_3\right\}. \end{aligned}$$

Now, applying the Filippov method described in Kuznetsov *et al.*, [58] we define

$$\sigma(x) = \left\langle \nabla H(x), f^{(1)}(x) \right\rangle \left\langle \nabla H(x), f^{(2)}(x) \right\rangle \tag{33}$$

being

$$H(x_1, x_2, x_3) = x_1 - x_3 \quad (\Rightarrow \nabla H = (1, 0, -1))$$

and

$$\begin{aligned} f^{(1)} &= \left(-rx_1 + qx_2, -qx_2 + b^{(1)}, k\alpha x_3\right) \\ f^{(2)} &= \left(-rx_1 + qx_2, -qx_2 + b^{(2)}, k\alpha(x_1, x_3)\, x_3\right) \\ &\left\langle \nabla H(x), f^{(1)}(x) \right\rangle \\ &\quad = -rx_1 + qx_2 - k\alpha x_3 \\ &\left\langle \nabla H(x), f^{(2)}(x) \right\rangle \\ &\quad = -rx_1 + qx_2 - k\alpha(x_1, x_3)\, x_3 \end{aligned} \tag{34}$$

All along Σ, we have $\alpha(x_1, x_3) = \alpha = 1$. Using (33) and (34) we then obtain:

$$\sigma(x) > 0 \tag{35}$$

and thus, we will have sliding dynamics according to [34].

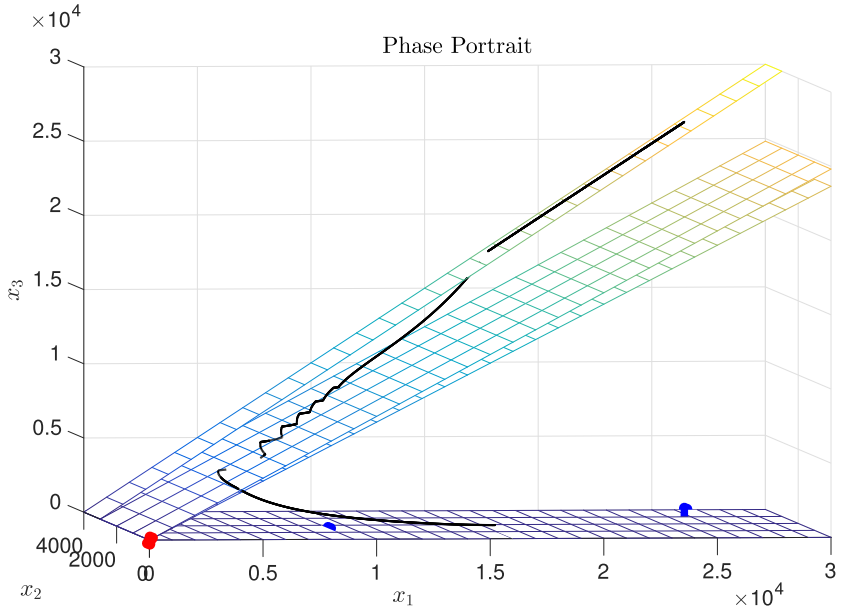

FIGURE 17. State space portrait showing the system dynamics undergoing crossing behaviors like a sewing or mend. $k > 0$.

Let us similarly explore the other switching manifolds. For general purposes we define $\Sigma_i \equiv \left\{x \in \mathbb{R}^3 : x_1 = h_i x_3\right\}$.

Therefore, on manifold Σ_i, we have

$$H_i(x_1, x_2, x_3) = x_1 - h_i x_3 \Rightarrow \nabla H_i = (1, 0, -h_i)$$

and

$$\begin{aligned} f^{(i)} &= \left(-rx_1 + qx_2, -qx_2 + b^{(i)}, k\alpha(x_1, x_3)\, x_3\right) \\ f^{(i+1)} &= \left(-rx_1 + qx_2, -qx_2 + b^{(i+1)}, k\alpha(x_1, x_3)\, x_3\right) \\ &\left\langle \nabla H_i(x), f^{(i)}(x) \right\rangle \\ &\quad = -rx_1 + qx_2 - h_i k\alpha(x_1, x_3)\, x_3 \\ &\left\langle \nabla H_i(x), f^{(i+1)}(x) \right\rangle \\ &\quad = -rx_1 + qx_2 - h_i k\alpha(x_1, x_3)\, x_3 \end{aligned} \tag{36}$$

Note that, if $x_1 = h_i x_3 \Leftrightarrow x_3 = \frac{1}{h_i} x_1$. Hence, (36) can be rewritten as (37).

$$\begin{aligned} \left\langle \nabla H_i(x), f^{(i)}(x) \right\rangle &= -rx_1 + qx_2 - h_i k\alpha\left(x_1, \frac{1}{h_i} x_1\right) x_3 \\ \left\langle \nabla H_i(x), f^{(i+1)}(x) \right\rangle &= -rx_1 + qx_2 - h_i k\alpha\left(x_1, \frac{1}{h_i} x_1\right) x_3 \end{aligned} \tag{37}$$

Again we obtain $\sigma(x) > 0$, meaning that the system crosses the switching manifolds (crossing phenomenon) like stitches in clothing.

To illustrate this conclusion, Fig. 17 shows a classical example of the *sewing* phenomenon. The Filippov analysis comprehensively and rigorously shows the system behavior around the switching manifolds.

V. CONCLUSIONS

This paper shows the nonlinear and piecewise-smooth dynamics exhibited by electricity-market models. It also integrated SD and DS approaches to better understand the onset of complex dynamics in such systems. Nonlinear analysis proved a handy tool for characterizing and describing the different phenomena exhibited by this kind of system. The asynchronous switching map has not been previously applied to electricity markets. Overall, the results reveal how a systematic analysis implementing hybrid techniques can identify and widely describe the threshold points in the system. This premise raises new questions on how the parameters influence the tipping points of the system.

Through a mathematical analysis of our proposed model and its generalization, we determined, classified, and described the threshold points of the electricity-market system in more detail than in previous studies [12], [17], [29], [30], and for all types of piecewise-smooth investment decisions. Consequently, we can explain the stable or unstable behaviors when the system is subjected to parameter variations. Through the systematic use of the proposed methodology, we can reconcile the SD and DS approaches for modeling, simulating and exploiting any SD-derived model. To this end, we need only to formulate the simulation model from a systems thinking or SD perspective. Combining our formulation with analysis tools that are traditionally used in DS and nonlinear dynamics theory (such as A-Switching Map), we can then explore the root of the system behaviors arising from the resulting differential equations.

The A-Switching Map tool facilitated the sensitivity analysis and revealed the modes of dynamic behavior for the determined parameter values. In the literature, we found no applications of A-Switching Map or similar methodologies

to economic and/or social systems. We also found that varying the *roi* changed the slopes of the switching manifold, implying that the *roi* and its associated parameters determine the threshold points of the system, thus influencing the market dynamics. In other words, the number of oscillations depends not on the initial conditions, but on how the solution approaches the switching manifolds.

Using together numerical and analytical tools (both traditionally and newly applied in this field) facilitated the supply-and-demand modeling of electricity markets, and the classification and modeling of non-smooth behaviors in the markets. Nevertheless, a qualitative analysis of market systems needs particular care, because the investment decisions are piecewise-smooth, and strong feedbacks emerge from the system structure. These systems may exhibit smooth behaviors, but also develop non-smoothness through the discontinuities.

The qualitative analysis of electricity-market models greatly benefited from the SD approach. It was concluded that both methodologies are complementary and might similarly benefit other applications. A mathematical study of the system equations arising from SD-based mental models is worthwhile, because the qualitative analysis of differential equations involves formalizing the individual processes in the SD. Therefore, such mathematical study can reveal scenarios and tipping points for decision-making in power markets. However, when applying the proposed approach two important issues should be considered: SD modelers need a mathematical background and generalize their models (only capture the main structure of the system) to avoid mathematical complexity.

Nevertheless, although computational effort can increase as system complexity increases, computational burden is not a big issue since nowadays we have access not only to high-performance computers, but also to high performance cloud computing.

Finally, for future work our proposed methodology will be applied to a case study to reveal and deeply describe the non-smooth dynamics of real energy systems and compare the results with other methodologies. Similar works, from a numerical point of view, have already demonstrated that the combination of SD/DS leads to discover counterintuitive behaviors and better understanding of SD models [12], [29].

APPENDIX

This Appendix proves the accumulation of the switching manifolds based on the definition of b.

$$b(inv) = \begin{cases} b_0 & \text{if} \quad D_{inv} \le d_0 \\ b_1 & \text{if} \quad d_0 < D_{inv} \le d_1 \\ b_2 & \text{if} \quad d_1 < D_{inv} \le d_2 \\ \vdots & \vdots \qquad\quad \vdots \\ b_{n-1} & \text{if} \quad d_{n-2} < D_{inv} \le d_{n-1} \\ b_n & \text{if} \quad D_{inv} > d_{n-1}. \end{cases}$$

$$\{b_i\}_{i=1}^{n}\,;\ b_i > 0 \quad \text{with} \quad 0 = b_0 < b_1 < \cdots < b_n$$
$$\{d_i\}_{i=1}^{n-1}\,;\ d_i > 0 \quad \text{with} \quad 0 = d_0 < d_1 < \cdots < d_{n-1}$$

Note that

$$h_1 < h_2 \Leftrightarrow \frac{1}{h_1} > \frac{1}{h_2}$$
$$1 - \mu + \log\left(\frac{a}{C_v - I - b} - 1\right) > 1 - \mu + \log\left(\frac{a}{C_{fv} d_1 + C_v - I - b} - 1\right)$$
$$\frac{1}{C_v - I - b} > \frac{1}{C_{fv} d_1 + C_v - I - b}$$

and that

$$C_{fv} d_1 > 0.$$

REFERENCES

[1] S. Gary and E. R. Larsen, "Improving firm performance in out-of-equilibrium, deregulated markets using feedback simulation models," *Energy Policy*, vol. 28, no. 12, pp. 845–855, Oct. 2000.
[2] D. W. Bunn and E. R. Larsen, "Sensitivity of reserve margin to factors influencing investment behaviour in the electricity market of england and wales," *Energy Policy*, vol. 20, no. 5, pp. 420–429, May 1992. [Online]. Available: https://www.sciencedirect.com/science/article/abs/pii/0301421592900638
[3] A. Ford, "Cycles in competitive electricity markets: A simulation study of the western united states," *Energy Policy*, vol. 27, no. 11, pp. 637–658, Oct. 1999. [Online]. Available: http://linkinghub.elsevier.com/retrieve/pii/S0301421599000506
[4] P. Ochoa and A. van Ackere, "Policy changes and the dynamics of capacity expansion in the swiss electricity market," *Energy Policy*, vol. 37, no. 5, pp. 1983–1998, May 2009. [Online]. Available: http://linkinghub.elsevier.com/retrieve/pii/S0301421509000500
[5] M. Bernardo, C. Budd, A. R. Champneys, and P. Kowalczyk, *Piecewise-smooth Dynamical Systems: Theory and Applications*, vol. 163. London, U.K.: Springer-Verlag, 2008.
[6] S. Jebaraj and S. Iniyan, "A review of energy models," *Renew. Sustain. Energy Rev.*, vol. 10, no. 4, pp. 281–311, Aug. 2006. [Online]. Available: http://linkinghub.elsevier.com/retrieve/pii/S1364032104001261
[7] A. M. Foley, B. P. Ó Gallachóir, J. Hur, R. Baldick, and E. J. McKeogh, "A strategic review of electricity systems models," *Energy*, vol. 35, no. 12, pp. 4522–4530, Dec. 2010. [Online]. Available: http://linkinghub.elsevier.com/retrieve/pii/S0360544210001866
[8] F. Teufel, M. Miller, M. Genoese, and W. Fichtner, "Review of system dynamics models for electricity market simulations," Work. Paper Ser. Prod. Energy, KIT, Karlsruhe, Germany, Tech. Rep. 2, 2013.
[9] S. Ahmad, R. M. Tahar, F. Muhammad-Sukki, A. B. Munir, and R. A. Rahim, "Application of system dynamics approach in electricity sector modelling: A review," *Renew. Sustain. Energy Rev.*, vol. 56, pp. 29–37, Apr. 2016.
[10] A. Borshchev and A. Filippov, "From system dynamics and discrete event to practical agent based modeling: Reasons, techniques, tools," in *Proc. 22nd Int. Conf. Syst. Dyn. Soc.*, vol. 22, 2004, pp. 25–29.
[11] R. A. Mehrabadi, M. P. Moghaddam, and M. K. Sheikh-El-Eslami, "Generation expansion planning in multi electricity markets considering environmental impacts," *J. Cleaner Prod.*, vol. 243, Jan. 2020, Art. no. 118611.
[12] J. D. Morcillo, F. Angulo, and C. J. Franco, "Analyzing the hydroelectricity variability on power markets from a system dynamics and dynamic systems perspective: Seasonality and ENSO phenomenon," *Energies*, vol. 13, no. 9, p. 2381, May 2020.
[13] R. F. Naill, "A system dynamics model for national energy policy planning," *Syst. Dyn. Rev.*, vol. 8, no. 1, pp. 1–19, 1992, doi: 10.1002/sdr.4260080102.
[14] I. Dyner, "Energy modelling platforms for policy and strategy support," *J. Oper. Res. Soc.*, vol. 51, no. 2, pp. 136–144, Feb. 2000. [Online]. Available: http://www.jstor.org/stable/254253

[15] J. D. Sterman, *Business Dynamics*, 1st Ed. New York, NY, USA: McGraw-Hill, 2000.
[16] A. Ford, J. Wright, and F. Prize, "System dynamics and the electric power industry," *Syst. Dyn. Rev.*, vol. 13, no. 1, pp. 57–85, 1997.
[17] J. Aracil, "On the qualitative properties in system dynamics models," *Eur. J. Econ. Social Syst.*, vol. 13, no. 1, pp. 1–18, 1999. [Online]. Available: http://www.edpsciences.org/10.1051/ejess:1999100
[18] M. Djemai and M. Defoort, "Hybrid dynamical systems," in *Solves Problems in the Analysis and Control of Hybrid Dynamical Systems* (Lecture Notes in Control and Information Sciences), vol. 457. Cham, Switzerland: Springer, 2015.
[19] S. Natsiavas, "Analytical modeling of discrete mechanical systems involving contact, impact, and friction," *Appl. Mech. Rev.*, vol. 71, no. 5, Sep. 2019.
[20] W. Znegui, H. Gritli, and S. Belghith, "Design of an explicit expression of the poincaré map for the passive dynamic walking of the compass-gait biped model," *Chaos, Solitons Fractals*, vol. 130, Jan. 2020, Art. no. 109436.
[21] T. Gedeon, "Multi-parameter exploration of dynamics of regulatory networks," *Biosystems*, vol. 190, Apr. 2020, Art. no. 104113.
[22] A. El Aroudi, D. Giaouris, H. H.-C. Iu, and I. A. Hiskens, "A review on stability analysis methods for switching mode power converters," *IEEE J. Emerg. Sel. Topics Circuits Syst.*, vol. 5, no. 3, pp. 302–315, Sep. 2015.
[23] V. Avrutin, Z. T. Zhusubaliyev, D. Suissa, and A. El Aroudi, "Non-observable chaos in piecewise smooth systems," *Nonlinear Dyn.*, vol. 99, no. 3, pp. 2031–2048, Feb. 2020.
[24] J. D. Morcillo, D. Burbano, and F. Angulo, "Adaptive ramp technique for controlling chaos and subharmonic oscillations in DC–DC power converters," *IEEE Trans. Power Electron.*, vol. 31, no. 7, pp. 5330–5343, Jul. 2016.
[25] L. Ma, X. Huo, X. Zhao, B. Niu, and G. Zong, "Adaptive neural control for switched nonlinear systems with unknown backlash-like hysteresis and output dead-zone," *Neurocomputing*, vol. 357, pp. 203–214, Sep. 2019.
[26] M. J. Grimble and P. Majecki, "Introduction to nonlinear systems modelling and control," in *Nonlinear Industrial Control Systems*. London, U.K.: Springer-Verlag, 2020, pp. 3–63.
[27] X. Wang and Y. Wang, "Novel dynamics of a predator-prey system with harvesting of the predator guided by its population," *Appl. Math. Model.*, vol. 42, pp. 636–654, Feb. 2017. [Online]. Available: http://www.sciencedirect.com/science/article/pii/S0307904X16305212
[28] H. Yoshioka and Y. Yaegashi, "Optimization model to start harvesting in stochastic aquaculture system," *Appl. Stochastic Models Bus. Ind.*, vol. 33, no. 5, pp. 476–493, Sep. 2017.
[29] J. D. Morcillo, C. J. Franco, and F. Angulo, "Simulation of demand growth scenarios in the colombian electricity market: An integration of system dynamics and dynamic systems," *Appl. Energy*, vol. 216, pp. 504–520, Apr. 2018. [Online]. Available: http://www.sciencedirect.com/science/article/pii/S0306261918302290
[30] J. M. Redondo, G. Olivar, D. Ibarra-Vega, and I. Dyner, "Modeling for the regional integration of electricity markets," *Energy Sustain. Develop.*, vol. 43, pp. 100–113, Apr. 2018. [Online]. Available: https://www.sciencedirect.com/science/article/pii/S097308261730220X
[31] V. D. Gil-Vera, "Forecasting Electricity Demand for Small Colombian Populations," *Cuaderno Activa*, vol. 7, no. 1, pp. 111–119, 2015.
[32] B. Brogliato, *Impacts in Mechanical Systems—Analysis and Modelling*, vol. 551. New York, NY, USA: Springer, 2000.
[33] J. Guckenheimer and P. Holmes, *Nonlinear Oscillations, Dynamical Systems, and Bifurcations of Vector Fields*, vol. 42. New York, NY, USA: Springer-Verlag, 2013.
[34] Y. Kuznetsov, *Elements of Applied Bifurcation Theory*. New York, NY, USA: Springer-Verlag, 2004.
[35] A. F. Filippov, *Differential Equations With Discontinuous Righthand Sides*. Norwell, MA, USA: Kluwer, 1988.
[36] M. di Bernardo and S. J. Hogan, "Discontinuity-induced bifurcations of piecewise smooth dynamical systems," *Phil. Trans. Roy. Soc. A, Math., Phys. Eng. Sci.*, vol. 368, no. 1930, pp. 4915–4935, Nov. 2010. [Online]. Available: http://rsta.royalsocietypublishing.org/content/368/1930/4915
[37] M. di Bernardo, A. R. Champneys, F. Garofalo, L. Glielmo, and F. Vasca, "Nonlinear phenomena in closed loop DC/DC buck converter," in *Proc. NDES (Nonlinear Dyn. Electron. Syst.)*, vol. 1, 1996, pp. 51–56.
[38] R. Leine, "Bifurcations in discontinuous mechanical systems of filippov-type," Ph.D. dissertation, Dept. Mech. Eng. Dyn. Control, Teknische Universiteit Eindhoven, The Netherlands, 2000.
[39] M. di Bernardo and F. Vasca, "Discrete-time maps for the analysis of bifurcations and chaos in DC/DC converters," *IEEE Trans. Circuits Syst. I, Fundam. Theory Appl.*, vol. 47, no. 2, pp. 130–143, Feb. 2000.
[40] A. P. Ivanov, "Impact oscillations: Linear theory of stability and bifurcations," *J. Sound Vibrat.*, vol. 178, no. 3, pp. 361–378, Dec. 1994.
[41] J. A. Amador, "Non-linear and non-smooth dynamics study in sustainable development systems," M.S. thesis, Departamento de Ingeniería Eléctrica, Electrónica y Computación, Universidad Nacional de Colombia, Bogotá, Colombia, 2011.
[42] N. Ghaffarzadegan and G. P. Richardson, "How small system dynamics models can help the public policy process," *Syst. Dyn. Rev.*, vol. 27, no. 1, pp. 22–44, 2011.
[43] J. W. Forrester, "System dynamics The next fifty years," *Syst. Dyn. Rev.*, vol. 23, no. 2, pp. 359–370, 2007.
[44] D. C. Lane and J. D. Sterman, "Profiles in operations research: Pioneers and innovators," in *Springer*, A. A. Assad and S. I. Gass, Eds. New York, NY, USA: Springer, 2011, ch. 20, pp. 363–386.
[45] J. Redondo, "Modelado de mercados de electricidad," Ph.D. dissertation, Departamento de Ingeniería Eléctrica, Electrónica y Computación, Universidad Nacional de Colombia, Bogotá, Colombia, 2012.
[46] XM. (2019). *Información Inteligente*. Accessed: Feb. 6, 2019. [Online]. Available: http://informacioninteligente10.xm.com.co/transacciones/Paginas/PrecioBolsa.aspx
[47] J. Weiss, "Market power and power markets," *Interfaces*, vol. 32, no. 5, pp. 37–46, Oct. 2002.
[48] L. Perko, *Differential Equations and Dynamical Systems*, vol. 7. New York, NY, USA: Springer-Verlag, 2013.
[49] L. Hirth, "What caused the drop in European electricity prices? A factor decomposition analysis," *Energy J.*, vol. 39, no. 1, pp. 1–16, Jan. 2018.
[50] S. Mosquera-López and A. Nursimulu, "Drivers of electricity price dynamics: Comparative analysis of spot and futures markets," *Energy Policy*, vol. 126, pp. 76–87, Mar. 2019. [Online]. Available: http://www.sciencedirect.com/science/article/pii/S0301421518307432
[51] Y. Barlas, "Formal aspects of model validity and validation in system dynamics," *Syst. Dyn. Rev.*, vol. 12, no. 3, pp. 183–210, 1996.
[52] H. Qudrat-Ullah and B. S. Seong, "How to do structural validity of a system dynamics type simulation model: The case of an energy policy model," *Energy Policy*, vol. 38, no. 5, pp. 2216–2224, May 2010.
[53] XM. (2019). *Información Inteligente*. Accessed: Feb. 27, 2019. [Online]. Available: http://informacioninteligente10.xm.com.co/demanda/paginas/default.aspx
[54] Z. R. Xiang and R. H. Wang, "Robust stabilization of switched non-linear systems with time-varying delays under asynchronous switching," *Proc. Inst. Mech. Eng., I, J. Syst. Control Eng.*, vol. 223, no. 8, pp. 1111–1128, Dec. 2009, doi: 10.1243/09596518JSCE809.
[55] R. A. Ibrahim, *Vibro-Impact Dynamics: Modeling, Mapping and Applications*, vol. 43. Berlin, Germany: Springer-Verlag, 2009.
[56] R. I. Leine, D. H. van Campen, and W. J. G. Keultjes, "Stick-slip whirl interaction in drillstring dynamics," *J. Vibrat. Acoust.*, vol. 124, no. 2, pp. 209–220, Apr. 2002.
[57] H. Fang and J. Xu, "Stick-slip effect in a vibration-driven system with dry friction: Sliding bifurcations and optimization," *J. Appl. Mech.*, vol. 81, no. 5, May 2014, Art. no. 051001.
[58] Y. A. Kuznetsov, S. Rinaldi, and A. Gragnani, "One-parameter bifurcations in planar filippov systems," *Int. J. Bifurcation Chaos*, vol. 13, no. 8, pp. 2157–2188, Aug. 2003. [Online]. Available: http://www.worldscientific.com/doi/abs/10.1142/S0218127403007874
[59] R. Verhoog, P. van Baal, and M. Finger, *System Dynamics Simulation to Explore the Impact of Low European Electricity Prices on Swiss Generation Capacity Investments*. Cham, Switzerland: Springer, 2018, pp. 31–61, doi: 10.1007/978-3-319-76867-0_3.
[60] M. Assili, M. H. J. D. B., and R. Ghazi, "An improved mechanism for capacity payment based on system dynamics modeling for investment planning in competitive electricity environment," *Energy Policy*, vol. 36, no. 10, pp. 3703–3713, Oct. 2008. [Online]. Available: http://www.sciencedirect.com/science/article/pii/S030142150800339X
[61] F. Olsina, F. Garcés, and H.-J. Haubrich, "Modeling long-term dynamics of electricity markets," *Energy Policy*, vol. 34, no. 12, pp. 1411–1433, Aug. 2006. [Online]. Available: http://www.sciencedirect.com/science/article/pii/S0301421504003325

JOHNNY VALENCIA-CALVO received the degree in electronics engineering and the M.Sc. degree in industrial automation from Universidad Nacional de Colombia, in 2010 and 2012, respectively, and the Ph.D. degree in computer sciences and decision, in 2016. His research experience has led him to become involved in topics related to dynamic analysis, nonlinear dynamics, and system dynamics, focusing on modeling, simulation, and applications of mathematics in engineering. Professional in computer science and decision, an Electronics Engineer from the National University of Colombia and, and a Master in industrial automation. He worked on the analysis, design, and modeling of a national electricity market to formulate new political strategies. Expert in systems dynamics and complex systems modeling.

GERARD OLIVAR-TOST (Member, IEEE) received the degree in mathematics from Universitat de Barcelona, Barcelona, España, in 1987, and the Ph.D. degree in science applied mathematics from Universitat Politècnica de Catalunya UPC, Barcelona, in 1997. He was with the Department of Applied Mathematics IV, UPC, for 17 years, as an Associate Professor. He is currently a Full Professor with the Department of Natural Sciences and Technology, University of Aysen, Chile. By that time, he was interested in nonlinear dynamics and chaos in DC-DC converters. He moved to Universidad Nacional de Colombia, Manizales, in 2005, where he was with the Department of Electrical and Electronics Engineering and Computer Science for ten years, as a Full Professor. He moved to the Faculty of Sciences, Department of Mathematics and Statistics, as a Full Professor, in 2015. He added to his interests' real applications of applied mathematics to health and development. He coordinates a Lab on engineering mathematics. He is the former and the President of COSIAM (Colombian Section of SIAM).

JOSÉ DANIEL MORCILLO-BASTIDAS received the degree in electronic engineering and the M.Sc. degree in industrial automation from the National University of Colombia, Manizales, in 2010 and 2012, respectively, and the Ph.D. degree in computer science from the National University of Colombia, Medellín, in 2018. He also worked as a Postdoctoral Researcher at the National University of Colombia, Manizales, in 2020. In 2010, he joined the Perception and Intelligent Control Group, and in 2014, he joined the Systems and Informatics Group, working in different I + D projects. He is currently working as a full-time Professor with the Engineering and Technologies Department, University of Monterrey, Mexico. His research interests include modeling, simulation, and control of power electronics and electricity markets, applying the theory of dynamical systems, system dynamics, and data analytics.

CARLOS JAIME FRANCO-CARDONA received the bachelor's degree in civil engineering and the Ph.D. degree in engineering. He is currently a Professor of complex systems with Universidad Nacional de Colombia. He also has experience in the electricity sector after working by ten years in ISA, a leading company in the wholesale Colombian Electricity Market. His current research interests are modeling systems, energy markets, and complexity.

ISAAC DYNER received the bachelor's degree in mathematics, the M.Sc. degree in statistics and operational research, and the Ph.D. degree in decision sciences from the University of London (LBS). He was an Associate Professor with Universidad Nacional de Colombia in the areas of operations research, system dynamics, strategy, regulation, and energy.